Jurnal Rekayasa Elektrika Vol. 20, No. 2, June 2024, page 43-48
ISSN. 1412-4785; e-ISSN. 2252-620X, Accredited by Kemendikbudristek No. 105/E//KPT/2022
DOI: 10.17529/jre.v20i2.33177

Scalability of MIMO Antennas: Assessing Gain and HPBW for Different Antenna Element Configurations

Salwa Salsabila*, Harfan Hian Ryanu, Levy Olivia Nur, and Bambang Setia Nugroho
Telkom University
Jl. Telekomunikasi No. 1 Terusan Buah Batu, Bandung, 40257
*e-mail: salwasalsabilaf@student.telkomuniversity.ac.id

Abstract—**The design of massive MIMO antennas presents challenges due to their large size, which can impede the design process. Additionally, the arrangement of multiple antenna elements in massive MIMO antennas poses a challenge, as it surpasses the capabilities of simulation software and involves complex procedures. Therefore, to address these issues, a scalability technique utilizing array factor theory is employed to determine the relationship between the configuration of MIMO antennas and the corresponding values of gain and half-power beamwidth (HPBW). By utilizing a simpler MIMO antenna array with incremental configurations, such as 2x2, 4x4, 8x8, and 16x16 MIMO element schemes, the array factor theory allows for the prediction of the gain and HPBW values for a massive MIMO antenna array with a specific configuration. This research aims to explore the scalability process and derive equations that relate the gain and HPBW values to the different MIMO configurations. The designed MIMO antenna arrangement is based on rectangular antennas with truncated corners and circular antennas with X slots, allowing for the investigation of various configurations operating at a frequency of 3.5 GHz.**

Keywords: ***gain, hpbw, massive MIMO antennas, mimo configurations, scalability***

I. INTRODUCTION

The growing demand for wireless communication and the increasing congestion of wireless bands due to data growth necessitate the development of a technology that can enhance data throughput. Consequently, researchers are faced with the challenge of finding a solution to address this issue. To cater to these needs, the Federal Communications Commission (FCC) has allocated frequency spectrum for 5G communication technology. The spectrum enables mobile internet-based electronic devices to benefit from higher throughput speeds compared to 4G technology, along with low latency that can be utilized in various cellular communication applications [1]. To leverage these advancements, massive MIMO antennas (massive MIMO) equipped with the Multiple Input Multiple Output (MIMO) system are employed as core technologies in the 5G communication system. The MIMO system utilizes multiple antennas for transmission, increasing channel capacity and signal strength while reducing the multipath effect. The implementation of massive MIMO, featuring a substantial number of antennas, has been proven to significantly enhance efficiency [2], [3].

The application of MIMO technology in antennas (MIMO antennas) introduces the occurrence of mutual coupling among individual antenna elements, as well as the presence of multipath components that can impact wave propagation. To address these challenges, it is essential to establish a high level of isolation between individual antenna elements [4]–[6]. Furthermore, careful consideration must be given to the configuration scheme of MIMO antennas during the design process. According to [7], simple MIMO antenna configurations (e.g., 2x2, 4x4) are not suitable for meeting the demands of 5G communication, which is predicted to offer speeds 1,000 times faster than 4G and improved reliability. Consequently, the design focus has shifted towards the massive MIMO antenna model to cater to the requirements of 5G communication. However, the design of massive MIMO antennas presents a challenge due to their larger physical dimensions, which can hinder the overall antenna design process [8]–[10].

Developing a large-scale antenna with a massive MIMO system poses a novel and distinct challenge within the realm of antenna simulation. In light of this, the authors suggest the adoption of Scalable Techniques to forecast the performance specifications of massive MIMO antennas, drawing upon the Array Factor (AF) theory alongside simple MIMO antennas.

The AF theory is utilized to compute the comprehensive antenna pattern, considering the distance and type of elements to facilitate scalability [11]. In a separate study [12], the influence of multiple elements on the AF in a uniform antenna arrangement is explored. Additionally, the investigation conducted by [13] examines the radiation parameters of extensive antenna arrays through the combination of AF and active element patterns. The findings also demonstrate a linear increase in the AF pattern with the increment in the number of antenna elements.

Received 17 July 2023; Revised 24 August 2023; Accepted 27 August 2023

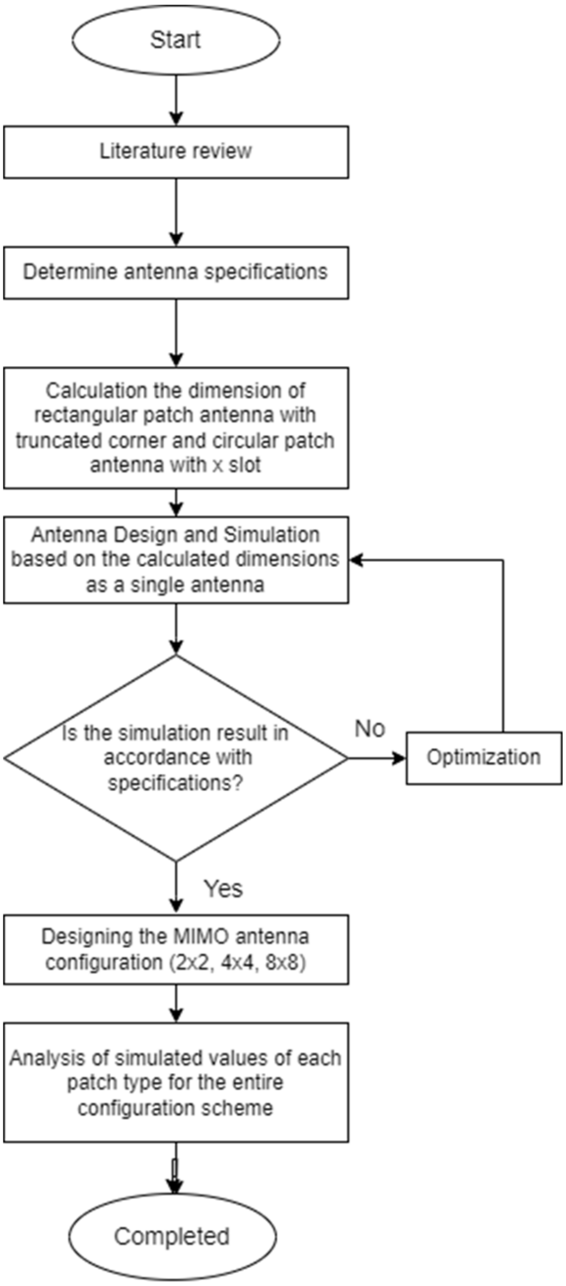

Figure 1. Research flow

II. METHOD

A. Configuration Schematic

The design method described in Figure 1 follows a systematic approach, beginning with a literature study to understand the concepts and theories related to the impact of using the truncated corner method on rectangular patch antennas and the effect of employing x-slots on circular antennas in the context of MIMO configuration. Once the concepts and theories are comprehended, the next step involves determining the specifications of the antennas. This entails calculating the antenna dimensions to meet the desired specifications prior to proceeding with the design and simulation process. The study comprises two stages: designing and simulating rectangular patch antennas with truncated corners and circular patch antennas with x-slots until the simulation results align with the specified requirements. Subsequently, the MIMO configuration is prepared incrementally, starting with 2x2 (4 antenna elements), followed by 4x4 (16 antenna elements) until 8x8 (64 antenna elements) while closely observing the increasing values and identifying any discernible patterns. The pattern of value increase is further analyzed and compared with the theoretical calculations of the array factor to ascertain the feasibility and effectiveness of the scalability technique.

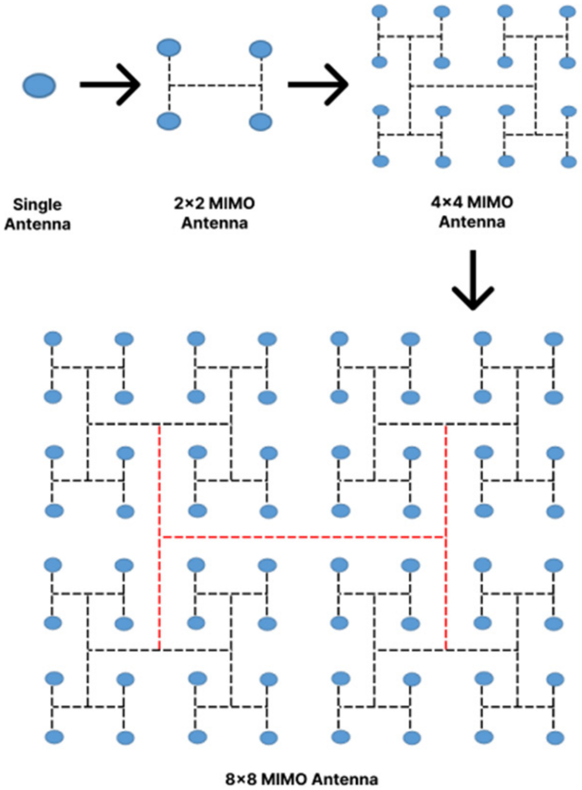

Figure 2. MIMO antenna configuration

By using the array factor theory to simulate the MIMO Antenna in stages, the pattern of growing the antenna elements is exponentially gradual with the configuration scheme as shown below.

The MIMO configuration in Figure 2 is simulated on two different patch types, namely Rectangular truncated corner patch antenna and Circular slotted x patch antenna. Each type of patch will be seen for its gain and HPBW results and then analyzed for changes in value for each configuration scheme.

B. Rectangular Truncated Corner Patch Antenna

The basic shape of this type of patch is a rectangular shape as shown in Figure 3 that is cut at an angle to produce a circular polarization type. This circular polarization can maintain the performance of antennas that are close to each other in a MIMO configuration. With circular polarization, the mutual coupling effect can be reduced to produce a high isolation value between adjacent antennas. The high

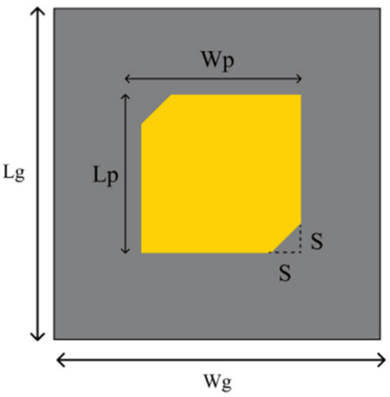

Figure 3. Rectangular truncated corner patch

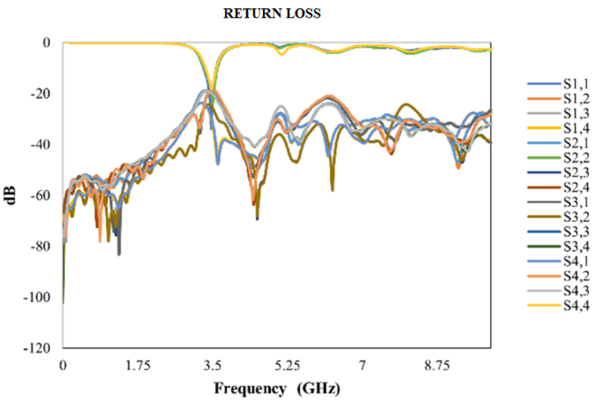

Figure 4. Return loss of rectangular 2x2 MIMO configuration

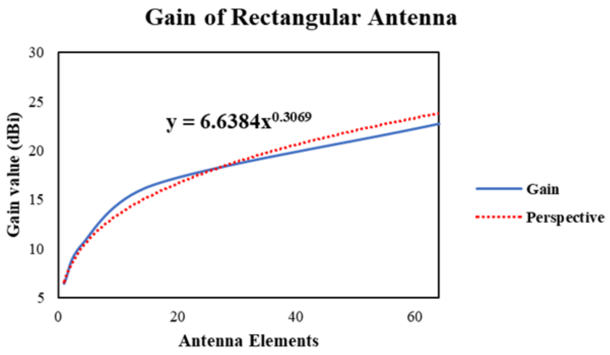

Figure 5. Gain value increment of rectangular antenna

Table 1. Gain value summary of rectangular antenna

MIMO Configurations	Gain (dB)	Percentage of Increase
Single Antenna	6.410	100%
2x2 MIMO	10.40	62.24%
4x4 MIMO	16.48	58.46%
8x8 MIMO	22.71	37.80%

Table 2. Angular width Summary of rectangular antenna

MIMO Configurations	HPBW	Percentage of Decrease
Single Antenna	95.1	100.00 %
2x2 MIMO	55.7	41.43 %
4x4 MIMO	26.6	52.24 %
8x8 MIMO	13.2	V

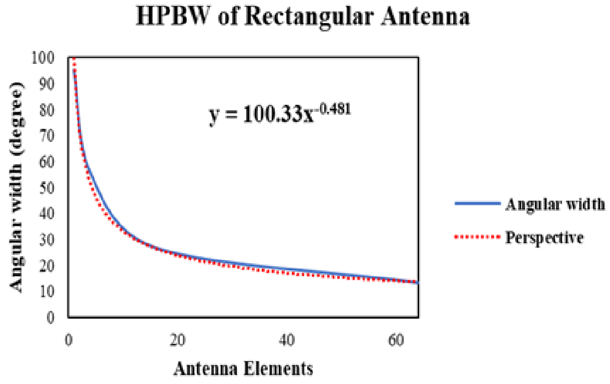

Figure 6. Angular width decrement of rectangular antenna

isolation value can be seen from the very small return loss value <<-10 dB.

Given the return loss results in the 2x2 configuration which shows the high isolation value as follows.

Based on Figure 4 above, it can be seen that the return loss value between adjacent antennas is very small so that the performance of each antenna does not have a bad influence on the other. After ensuring high isolation between adjacent antennas, proceed to find out the resulting gain and HPBW values.

The gain and HPBW values studied are the simulated gain values of each configuration starting from a single antenna, 2x2 MIMO, 4x4 MIMO, and 8x8 MIMO. The increased value in each configuration's findings is listed in the Table 1.

Based on Table 1, a graph is used to illustrate the rise in gain value for each configuration stage and then inferences are made in the form of an equation, as shown in the picture below.

Figure 5 illustrates the relationship between the increase in gain value and the number of antenna elements, which corresponds to the data listed in Table 1. From the figure, as more antenna elements are used, the gain value also increases. This shows that there is a positive relationship between the number of antenna elements and the gain value. Thus, a mathematical equation can be used to calculate the gain value with a larger number of antenna elements than those listed in Table 1. Through the use of the equation, it can be predicted that increasing the number of antenna elements will result in an even greater increase in the gain value. As such, these results provide a deeper understanding of how the use of more antenna elements can improve system performance and obtain higher gain.

Additionally, the values in the following table are used to examine the HPBW angle.

Based on Table 2, the decrease in HPBW angle for each configuration stage is represented in the form of a graph to then conclude as follows:

Figure 6 illustrates the relationship between the decrease in Half Power Beamwidth (HPBW) angle and the number of antenna elements, which corresponds to the data contained in Table 2. From the figure, the more antenna elements used, the smaller the HPBW angle. This

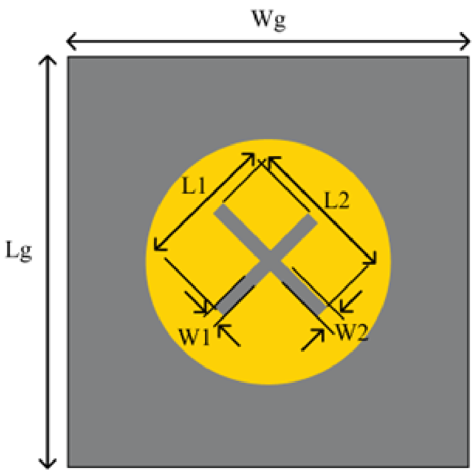

Figure 7. Circular slotted X patch

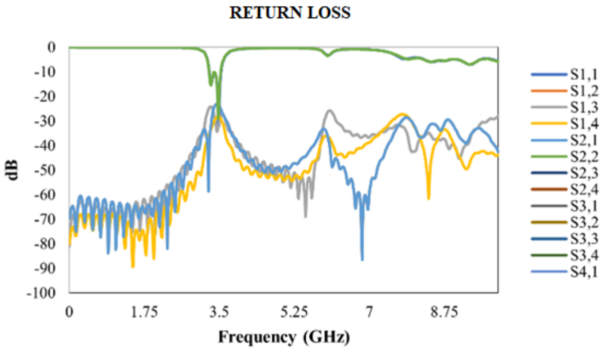

Figure 8. Return loss of circular 2x2 mimo configuration

Table 3. Gain value summary of circular antenna

MIMO Configurations	Gain (dB)	Percentage of Increase
Single Antenna	6.561	100.00 %
2x2 MIMO	10.79	64.45 %
4x4 MIMO	16.85	56.16 %
8x8 MIMO	22.9	35.91%

indicates a negative relationship between the number of antenna elements and the HPBW angle. Using the mathematical equations generated from the data in Table 2, we can calculate the HPBW angle with a larger number of antenna elements than listed in the table. Using the equation, it can be predicted that increasing the number of antenna elements will result in an even narrower HPBW angle. These results provide a deeper understanding of how an increase in the number of antenna elements can lead to improved precision of radiation direction and signal focus to a narrower area in the antenna system.

C. Circular Slotted X Patch Antenna

The basic shape of this type of patch as shown in Figure 7 is a circular shape that is given an X shape cut to produce a circular polarization type. Given the return loss results in the 2x2 configuration which shows a high isolation value.

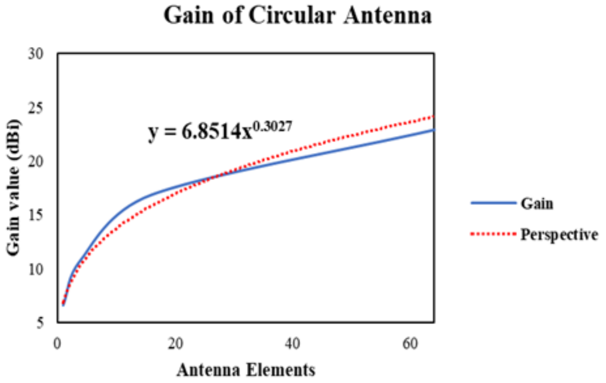

Figure 9. Gain value increment of Circular Antenna

Table 4. Angular width summary of circular antenna

MIMO Configurations	HPBW	Percentage of Decrease
Single Antenna	92.1	100.00 %
2x2 MIMO	54.4	39.52 %
4x4 MIMO	26.1	52.24 %
8x8 MIMO	12.9	51.50%

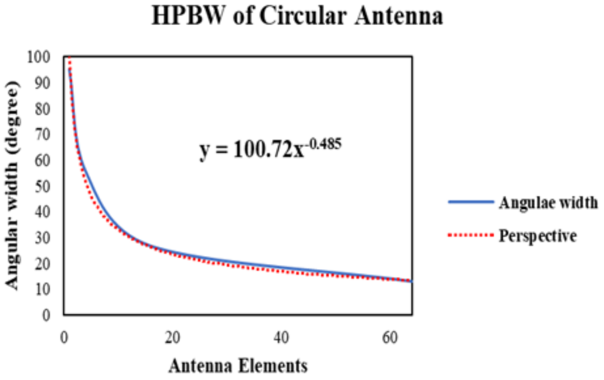

Figure 10. Angular width decrement of circular antenna

According to Figure 8 above, the return loss value between adjacent antennas is relatively low, ensuring that the performance of each antenna does not adversely affect the performance of the others. Determine the resulting gain and HPBW values after ensuring high isolation between nearby antennas.

The simulated gain values for each configuration, starting with a single antenna, 2x2 MIMO, 4x4 MIMO, and 8x8 MIMO, were used to determine the gain and HPBW values. The findings of the gain value in each setup scheme are listed in Table 3

Based on Table 3, a graph is used to show the rise in gain value for each configuration step before conclusions are made in the form of an equation, as shown in Figure 9. Similar to the rectangular shape, the circular shape also has a pattern of increasing gain as the antenna element increases as shown in Figure 9 above.

Additionally, the values in the following table are used to examine the HPBW angle. Based on Table 4, the decrease in HPBW angle for each configuration stage is represented in the form of a graph to then draw conclusions in the form of equations as shown in Figure 10.

As with the HPBW angle, the pattern of the angle decrease is consistent in both the rectangular and circular shapes. In the circular shape, the angle decrease can be seen as shown in Figure 10.

III. RESULTS AND ANALYSIS

The gain value of the rectangular antenna is directly proportional to the number of antenna elements, forming a curve that can be expressed using the formula $y=6.6384x^{0.3069}$ while the gain value of the circular antenna is linearly proportional to the number of antenna elements, forming a curve that can be expressed using the formula $y=6.8514x^{0.3027}$.

In the Rectangular Antenna, the gain (y) increases at a rate set by the exponent (0.3069). x's value determines how exponentially the gain grows. The second is the gain value of circular antenna gain (y) also increases at a rate that depends on the exponent (0.3027). However, the differences in the coefficient a value (6.6384 and 6.8514) indicate a change in the gain's starting value at the same x value. Both equations exhibit a typical exponential gain improvement pattern. The value of x (number of MIMO antenna elements) affects the gain obtained.

The two equations each depict the exponential relationship between the number of MIMO antenna elements (x) and gain (y) in dBi. According to the equation of Circular Antenna Bigger Exponent, the gain increases more quickly than it did in the equation of Rectangular Antenna as the number of MIMO antenna elements increases. With higher values of x, a greater gain can be realized. However, the rate of gain growth slows down as the number of antenna elements increases. The equation demonstrates how the number of antenna elements utilized may have an impact on the gain improvement of a MIMO system. Because the coefficient values in the two equations differ, it is likely that the initial gain value at the same number of antennas will also differ slightly. Gain increases for a given number of antenna elements are also influenced by the characteristics of the used antenna, such as its frequency response, radiation pattern, and efficiency.

It is important to keep in mind that the gain in dBi compares to the ideal isotropic antenna, which emits light uniformly in all directions. The equation can be used to determine a MIMO system's gain based on the anticipated number of antenna elements. Analysis of this gain pattern is essential during design and optimization for MIMO systems to function as intended. The equation makes it possible to compare the performance of MIMO systems with different numbers of antenna elements, allowing one to select the number of antenna components that best satisfies the needs of a particular application.

The HPBW angle of a circular antenna is directly proportional to the number of antenna elements, whereas the HPBW angle of a rectangular antenna is inversely proportional to the growth in the number of antenna components, forming a curve that can be calculated using a formula. The curve that comes from this relationship can be defined by the following formula. The HPBW angle (y) in both equations decreases as the natural logarithm of the x value (number of MIMO antenna elements) increases. The HPBW angle decreases as x increases in value. The two equations' different coefficient and constant values reveal the two different rates at which the HPBW angle decreases at the same x value. As the value of x (number of MIMO antenna elements) increases, both equations exhibit a slow pattern of decreasing HPBW angle, showing that the HPBW angle declines more slowly as the number of MIMO antenna elements used rises. In degrees, the HPBW angle is expressed.

Different values of the coefficients and constants in the equations could lead to differences in the amount of gain increase or HPBW angle drop in both analyses throughout a range of x values (number of MIMO antenna elements). It should be mentioned that the radiation pattern and focus of MIMO antennas with different element counts can be determined from the relative measurements of gain (measured in dBi) and HPBW angle (measured in degrees).

The equation illustrates the logarithmic relationship between the number of MIMO antenna elements (x) and the HPBW angle (y) in degrees. The graph shows the relationship between an increase in antenna element count and a decrease in HPBW angle. The antenna radiation pattern width at the half-peak of the radiated power is described by the HPBW angle. The circular patch equation shows a slower fall in HPBW angle than the initial equation because of the difference coefficient values (100.33 and -100.72). With an increase in x (number of MIMO antenna elements), the HPBW angle decreases, indicating a sharpening of the radiation pattern. The circular patch equation's slower HPBW angle drop shows that adding more antenna elements has less of an effect on the radiation pattern's ability to be constricted than the rectangular patch equation. The variance of the HPBW angle corresponds to the variance of the constants in the two equations for the same number of antenna elements. It is critical to keep in mind that the antenna design, including its form, desired radiation pattern, and frequency bandwidth, can also have an impact on a MIMO antenna's radiation pattern.

The HPBW angle of the MIMO system can be determined using the equation based on the anticipated number of antenna elements. To maintain signal directionality and reduce antenna interference, it is essential to study the HPBW angle drop pattern while constructing MIMO systems. These equations can be used in further research to compare the effectiveness of MIMO systems with different numbers of antenna elements. In order to produce the needed radiation pattern, lessen antenna interference, and boost system effectiveness, the appropriate number of antenna elements must be determined.

IV. CONCLUSION

In conclusion, the research findings indicate that the gain of rectangular and circular antennas in a MIMO configuration is influenced by the number of antenna elements. The gain increases exponentially with the number of elements, but the growth rate is slightly higher for rectangular antennas compared to circular antennas. The equations derived for gain provide a mathematical representation of the gain improvement pattern. Additionally, the half-power beamwidth (HPBW) angle decreases with the increase in antenna elements for rectangular antennas, while it increases linearly for circular antennas. The equations for the HPBW angle demonstrate the relationship between the number of antenna elements and the angle. The rate of decrease or increase in the HPBW angle varies based on the coefficients and constants in the equations. These equations are valuable in understanding the radiation pattern and performance characteristics of MIMO antennas. They can aid in selecting the appropriate number of antenna elements and optimizing the MIMO system for specific application requirements.

REFERENCES

[1] H. L. Chu, G. Mishra, and S. K. Sharma, "Dual polarized wideband vivaldi 4x4 subarray antenna aperture for 5G massive MIMO panels with simultaneous multiple beams," in Proc. International Symposium on Antenna Technology and Applied Electromagnetics, 2018, pp. 1–2.

[2] S. A. Khwandah, J. P. Cosmas, P. I. Lazaridis, Z. D. Zaharis, and I. P. Chochliouros, "Massive MIMO systems for 5G communications," *Wireless Personal Communications*, vol. 120, no. 3, pp. 2101–2115, 2021.

[3] N. H. M. Adnan, I. M. Rafiqul, and A. H. M. Z. Alam, "Massive MIMO for fifth generation (5G): opportunities and challenges," Proc. International Conference on Computer and Communication Engineering, 2016, pp. 47–52.

[4] S. S. Jehangir and M. S. Sharawi, "A Miniaturized UWB Bi-Planar Yagi-Like Antenna," in Proc. International Symposium on Antennas and Propagation & USNC/URSI National Radio Science Meeting, 2017, pp. 501–502.

[5] H. Zhai, J. Zhang, Y. Zang, Q. Gao, and C. Liang, "An LTE base-station magnetoelectric dipole antenna with anti-interference characteristics and its MIMO system application," *IEEE Antennas and Wireless Propagation Letters*, vol. 14, pp. 906–909, 2015.

[6] S. Biswas, K. Singh, O. Taghizadeh, and T. Ratnarajah, "Coexistence of MIMO radar and FD MIMO cellular systems with QoS considerations," *IEEE Transactions on Wireless Communications,* vol. 17, no. 11, pp. 7281–7294, 2018.

[7] Y. Li, C. Y. D. Sim, Y. Luo, and G. Yang, "12-Port 5G massive MIMO antenna array in sub-6GHz mobile handset for LTE bands 42/43/46 applications," *IEEE Access*, vol. 6, pp. 344–354, 2017.

[8] Y. W. Andika, H. Putri, and D. A. Nurmantris, "Antena transceiver untuk komunikasi bluetooth ISM-band dengan metode complementary split ring resonator," *Jurnal Rekayasa Elektrika*, vol. 14, no. 2, 2018.

[9] I. Surjati, S. Alam, and S. Hotman, "Polarisasi melingkar antena mikrostrip E shape dengan pencatu electromagnetic coupling," *Jurnal Rekayasa Elektrika*, vol. 13, no. 1, pp. 35, 2017.

[10] A. P. Prakusya, D. A. Nurmantris, and R. A. -, "Antenna MIMO 4 elemen untuk komunikasi 5G pada frekuensi 3.5 GHZ," *Jurnal Rekayasa Elektrika*, vol. 18, no. 3, pp. 158–164, 2022.

[11] J. N. Sahalos, "Design of shared aperture radar arrays with low sidelobe level of the two-way array factor," *IEEE Transactions on Antennas and Propagation,* vol. 68, no. 7, pp. 5415–5420, 2020.

[12] B. Molaei and A. A. Kishk, "Non-reciprocity view of the MIMO antenna arrays in transmitting and receiving modes using the maximized unique receiving pattern theory resulted by angle-wise array factor," *IEEE Access*, vol. 8, pp. 100280–100287, 2020.

[13] F. Yang, S. Yang, W. Long, Y. Chen, S. Qu, and J. Hu, "A novel 3-d-nufft method for the efficient calculation of the array factor of conformal arrays," *I IEEE Transactions on Antennas and Propagation,* vol. 69, no. 10, pp. 7047–7052, 2021.